Article

On the Range Equation for Hybrid-Electric Aircraft

Aman Batra [1],*, Reiko Raute [2] and Robert Camilleri [1]

1 Institute of Aerospace Technologies, University of Malta, MSD2050 Msida, Malta
2 Department of Industrial Electrical Power Conversion, University of Malta, MSD2050 Msida, Malta
* Correspondence: aman.batra@um.edu.mt

Abstract: This paper proposes a new range equation for hybrid-electric aircraft. The paper revisits the theory of the range equation for a hybrid-electric aircraft with constant power split published earlier in the literature and proposes a new efficiency-based definition of the degree of hybridization (φ), one which includes the efficiencies of the electric or fuel-powered drivetrain. The paper shows that the efficiencies of the respective drivetrains play a significant role in the range estimation of the hybrid-electric aircraft. The paper makes use of a case study to show the relationship between battery energy density, powertrain efficiency and modification in the definition of the degree of hybridization φ with aircraft range. We show that for every aircraft design, there is a battery energy density threshold, for which the aircraft range becomes independent of the degree of hybridization. Below this threshold, the range decreases with an increase in the degree of hybridization. Conversely, beyond this threshold, the aircraft range increases with the degree of hybridization. Our study finds that the new definition of φ has shifted this threshold significantly upwards compared to earlier publications in the literature. This makes the design of an aircraft with a high degree of hybridization less optimistic.

Keywords: hybrid-electric; aircraft range; battery energy density; efficiency-based degree of hybridization

1. Introduction

This paper reexamines the theoretical range equation for a hybrid-electric aircraft with a constant power split. The paper introduces an efficiency-based hybridization ratio between the power supplied by the electrical drivetrain and the fuel-powered system. As the world faces rapid climate change, there is an urgent need to reduce emissions. While aviation contributes to about 3% of global emissions, only 10% of the global population has access to flight. As the world economy continues to grow and more countries are pulled out of poverty, these, too, would like to travel. Aviation is hence expected to return to its pre-COVID growth rate of around 3–4% per annum [1]. For a few decades, the European Union has had a very ambitious strategy documented in Flightpath 2050 [2]. This aimed to achieve sustainable air travel while continuing to serve society's demands. The strategy sets aggressive targets to reduce in-flight CO_2 emissions by 70%, NO_x emissions by 90% and a reduction in noise when compared to the year 2000 [2]. These goals are now being reinforced through the Green Deal, which aims to shift this sector to net zero emissions in the shortest timeframe possible. To achieve this goal, several solutions are being researched, such as Electrified aircraft [3], hydrogen-based aircraft [4] and Sustainable Aviation Fuel (SAF) [5].

With the currently available technology, electrochemical battery energy densities are about 40 times less than that of Kerosene. With the present battery energy density of around 228 Wh/kg for Lithium-Ion batteries, a fully-electric aircraft can only manage a shorter range and very limited payload. With the current progress in battery technology, the energy density of batteries doubles every 23 years [6], so it is unlikely that a fully electric large transport aircraft will be developed soon. Likewise, hydrogen-aircraft still has many unanswered questions. While there is a significant effort to address the challenges related

to aircraft design, there are additional challenges to develop the fuel infrastructure and provide the industry with green hydrogen. Conversely, SAF may reduce the demand for oil-based fuels but will not reduce the carbon footprint rapidly. There is also a significant challenge on how to shift towards SAF without affecting the price of food [7]. This paper, therefore, focuses on hybrid aircraft, which may offer a short-midterm solution for reducing emissions. This may fill the gap and provide a solution until these uncertainties are resolved, and a long-term solution is found.

This paper focuses on the theory of electrified aircraft, particularly hybrid-electric aircraft [8–10]. Parameters such as range and endurance, which give the distance covered on the ground and time taken for a particular mission, provide important information about the aircraft's performance. The theory to establish the range for a traditional fuel aircraft is classically referred to as the Breguet range equation [11,12], which is named after a French aircraft designer and was derived by J G Coffin in 1920. Conversely, the range equation for fully electric aircraft has been derived [13] and is also well accepted. However, the range equation for hybrid-electric aircraft is still debated. Ravishankar and Chakravarthy [14] divide the range equation into different regimes based on the power available to the power required to propel an aircraft. However, their range expression does not take into consideration the logarithmic term, which is a result of the fuel being consumed throughout the flight. Their derivation erroneously considers a constant fuel mass-flow rate throughout the mission. Elmousadik et al. [15], in their work, exhaust one energy source (fuel) initially and then switch to the other energy source (batteries) later in the mission. This aids in increasing the range of the aircraft as the weight reduces, but it also leads to significant sizing of the engine components for 100% functioning. Rohacs and Rohacs [16] deduce their own range equation and also introduce a new performance factor, namely the energy factor (i.e., energy used per unit work), which is used to compare aircraft with different propulsion systems. Additionally, while their range equation reaches the fully-fuelled aircraft range at the limiting case ($\varphi = 0$), at the full-electric limiting case ($\varphi = 1$), it does not reach the all-electric aircraft range equation. Some of the derived range expressions have separate components for different energy sources, where the weight of one component (fuel) decreases, and the other (batteries) remains the same [17,18]. However, the straightforward addition of the two ranges (for fully-fuelled and all-electric) will not suffice as the conditions in both cases are distinct. Recently, Vries et al. [11] published a range equation for a constant power split. Their derivation for a hybrid-electric aircraft with a constant power, split satisfy both limiting cases. Thus, for $\varphi = 0$, the hybrid-electric equation is reduced to the Breguet equation, while for $\varphi = 1$, the hybrid equation is reduced to the electric range equation.

The authors of this paper revisit this derivation and propose an efficiency-based definition of the term (φ), which describes the degree of hybridization. φ is defined as the division in the energy extracted from the fuel source and battery source. This, in turn, impacts the derivation of the range equation. The authors are of the opinion that the original definition of φ is inaccurate as it ignores the efficiencies of the respective drivetrains from which power is being extracted. The paper shows how this change has a significant effect on the development of the battery component in a hybrid-electric aircraft. To achieve this, the paper is organized in the following manner: The subsequent Section 2 gives an introduction to the various hybrid-electric aircraft configurations. The paper sticks to the conventions that have already been established in earlier literature. The following Section 3 presents the new definition of the term degree of hybridization (φ), which is efficiency-based. Section 4 elucidates the derivation of the modified range equation in a comprehensive manner. The limiting cases for when $\varphi = 0$ (fuel aircraft) and $\varphi = 1$ (full electric aircraft) are also described. The paper shows that the newly derived range equation for the hybrid-electric aircraft is reduced to the classical Breguet equation for $\varphi = 0$ and the electric range equation for $\varphi = 1$. Section 5 presents the case study, which is worked on the modified range equation. The final Section 6 provides a Discussion and Conclusion,

highlighting the impact of the new definition of φ on the overall hybrid-electric range equation.

2. Hybrid-Electric Aircraft Configuration

Hybrid-electric propulsion systems exist in different configurations, with the most common being series hybrid and parallel hybrid [19,20]. The basis of classification is the mode of power delivery to the propeller. In a series hybrid powertrain, the propeller is always driven by an electrical motor. This can then be supplied by a battery or electrically fed by a generator which is in turn driven by a fuel-powered gas turbine. Sometimes, series hybrid-electric architectures are depicted without a battery source (known as a turbo-electric architecture [21,22]); in that case, there would be considerable emissions as the gas turbine would be running for the entire operation.

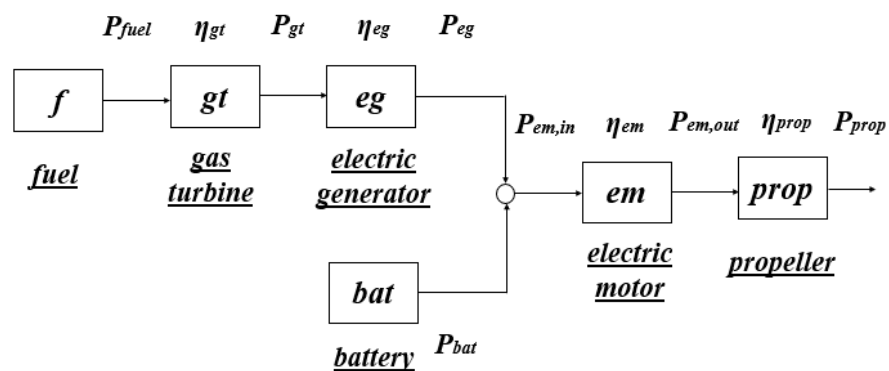The series hybrid-electric powerplant is depicted in Figure 1.

Figure 1. Schematic of the series hybrid-electric powerplant [11].

The symbols in the figure are defined as follows: *gt* is the gas turbine, *eg* is the electric generator, *bat* is the battery, *em* is the electric motor, *prop* is the aircraft propeller, *f* stands for the fuel, P denotes power and η is the efficiency. Conversely, in a parallel-hybrid powertrain, the propeller is connected to a gearbox which is fed either by the gas turbine, the electric motor powered by a battery or a combination of both. The gearbox is an addition in this paper, which was not considered in [11]. The parallel hybrid-electric powerplant is depicted in Figure 2.
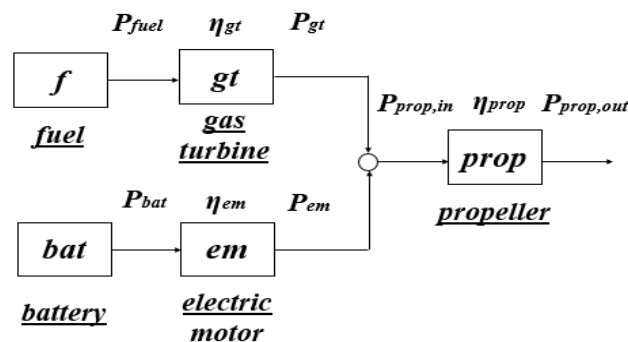

Figure 2. Schematic of the parallel hybrid-electric powerplant [11].

The symbols in the figure are defined as follows: *f* stands for the fuel, *gt* is the gas turbine, *bat* is the battery, *em* is the electric motor, *prop* is the aircraft propeller, P denotes power and η is the efficiency. These configurations can be generalized to the schematic shown in Figure 3. The general definitions of the efficiencies for series and parallel hybrid-electric configurations are explained in Table 1.
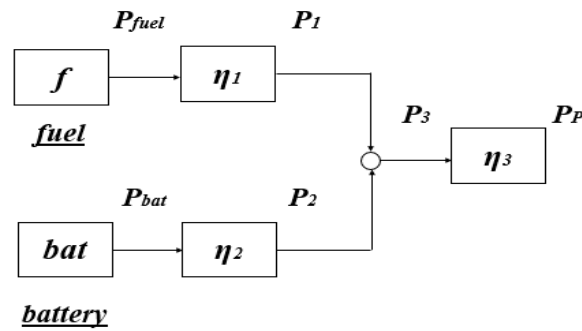
Figure 3. Schematic of a simplified hybrid-electric powerplant representation [11].

Table 1. Relation between efficiencies for series and parallel hybrid-electric configuration.

Simplified Representation	Mechanical-Node Architecture (or Parallel Configuration)	Electrical-Node Architecture (or Series Configuration)
η_1	η_{gt}	$\eta_{gt}\eta_{eg}$
η_2	η_{em}	1
η_3	$\eta_{gb}\eta_p$	$\eta_{em}\eta_{gb}\eta_p$

The following section gives a new efficiency-based definition of φ.

3. An Efficiency-Based Definition of the Degree of Hybridization (φ)

According to the general schematic shown in Figure 3, φ should be split at the node so that a portion of the power is supplied through the mechanical drivetrain while another portion is supplied through the electrical drivetrain. The definition of the power split is shown in Equation (1). The mechanical power P_1 is a result of the energy available at the fuel source and the efficiency of converting this into work. Likewise, the electrical power P_2 is a result of the energy stored in the battery and the efficiency of converting this into work. Without considering the efficiencies of the components (as was the case in [11]), the power is not split adequately, and the definition remains incomplete. A new efficiency-based definition for the degree of hybridization is shown in Equation (2).

$$\varphi = \frac{P_2}{P_1 + P_2} \tag{1}$$

$$\varphi = \frac{P_{bat}\eta_2}{P_f\eta_1 + P_{bat}\eta_2} \tag{2}$$

where φ is the degree of hybridization, P_{bat} is the power from the battery source, P_f is the power from the fuel source and η_1, η_2 and η_3 are the efficiencies for the two paths and the combined path, respectively. With this new definition, the range equation is also impacted, and therefore the next section provides the derivation of the modified range equation. It also describes how the new equation satisfies the limiting cases $\varphi = 0$ and $\varphi = 1$.

4. Derivation of Modified Hybrid-Electric Range Equation

The derivation is carried out assuming a steady-level flight. Therefore, the lift is equal to the weight, and the drag is equal to the thrust. The flight path angle is considered to be very small and can be neglected in this case. These assumptions are similar to those taken in the derivation of the Brequet equation for a conceptual design process of a conventional fuel-powered aircraft [12]. More elaborate range calculations can be found later in the design process using the mission profile. For a steady, level flight:

$$L = W \tag{3}$$

$$T = D \tag{4}$$

$$L = \frac{1}{2}\, \rho\, v^2\, S\, c_L \tag{5}$$

$$D = \frac{1}{2}\, \rho\, v^2\, S\, c_D \tag{6}$$

where L is the lift, D is the drag, W is the weight of the aircraft, c_L is the coefficient of lift, c_D is the coefficient of drag, T is the thrust, ρ is the density of air at that altitude, S is the wing area and V is the cruise speed. From the above equations:

$$T = \frac{W}{\frac{c_L}{c_D}} \tag{7}$$

The propulsive power P_p is defined as a product of the thrust T and the aircraft velocity as:

$$P_p = T\, v \tag{8}$$

Rearranging the Equation (2), we get:

$$P_{bat} = \left(\frac{\varphi}{1-\varphi}\right)\left(\frac{\eta_1}{\eta_2}\right) P_f \tag{9}$$

where P_f is the power from fuel, P_{bat} is the power from the battery, η_1, η_2 and η_3 are the efficiencies from Figure 3. The power balance at the node in Figure 3 can be written as:

$$\frac{P_p}{\eta_3} = \eta_1(P_f) + \eta_2(P_{bat}) \tag{10}$$

Also, the energy contained in the fuel source and battery source depletes over the flight time.

$$P_f = -\frac{dE_f}{dt} \tag{11}$$

$$P_{bat} = -\frac{dE_{bat}}{dt} \tag{12}$$

where E_f is the energy from fuel, E_{bat} is the energy from the battery. Inserting in Equations (9) and (10), we get:

$$\frac{P_p}{\eta_3} = \eta_1\left(-\frac{dE_f}{dt}\right) + \eta_2\left(-\frac{dE_{bat}}{dt}\right) \tag{13}$$

$$\frac{dE_{bat}}{dt} = \left(\frac{\varphi}{1-\varphi}\right)\left(\frac{\eta_1}{\eta_2}\right)\frac{dE_f}{dt} \tag{14}$$

Putting values from Equations (8), (9) and (14) in (13), we get:

$$\frac{T\, v}{\eta_3} = \eta_1\left(-\frac{dE_f}{dt}\right) + \eta_2\left(-\frac{dE_{bat}}{dt}\right) \tag{15}$$

$$\frac{W\, v}{\eta_3\, \frac{c_L}{c_D}} = \left(-\frac{dE_f}{dt}\right)\left(\eta_1 + \eta_2\frac{\varphi}{1-\varphi}\left(\frac{\eta_1}{\eta_2}\right)\right) \tag{16}$$

Rearranging the above equation, we get:

$$v = -\eta_1 \eta_3 \frac{c_L}{c_D} \frac{1}{W} \left(\frac{dE_f}{dt} \right) \left(1 + \frac{\varphi}{1 - \varphi} \right) \tag{17}$$

The aircraft range R can be found by:

$$R = \int_{t_{start}}^{t_{end}} v * dt \tag{18}$$

Using the value of velocity from Equation (17), we obtain:

$$R = -\eta_1 \eta_3 \frac{c_L}{c_D} \left(1 + \frac{\varphi}{1 - \varphi} \right) \int_{t_{start}}^{t_{end}} \frac{1}{W} \left(\frac{dE_f}{dt} \right) dt \tag{19}$$

Due to the fuel load reduction throughtout the flight, the total aircraft weight varies over time and can be defined as:

$$W(t) = W_{OE} + W_{PL} + W_{bat} + W_f(t) \tag{20}$$

where W_{OE} is the empty weight of the aircraft, W_{PL} is the payload weight of the aircraft, W_{bat} is the weight of the battery and W_f is the weight of the fuel. Also:

$$W_f(t) = \frac{g}{e_f} E_f(t) \tag{21}$$

$$W_{bat}(t) = \frac{g}{e_{bat}} E_{0,bat} \tag{22}$$

where e_f is the energy density of the fuel and e_{bat} is the energy density of the battery.

Using values from Equations (20)–(22), we obtain:

$$R = -\eta_1 \eta_3 \frac{c_L}{c_D} \left(1 + \frac{\varphi}{1 - \varphi} \right) \int_{t_{start}}^{t_{end}} \frac{\left(\frac{dE_f}{dt} \right)}{\left(W_{OE} + W_{PL} + \frac{g}{e_{bat}} E_{0,bat} + \frac{g}{e_f} E_f(t) \right)} dt \tag{23}$$

The limits of the integral are inverted, and the minus sign is removed:

$$R = \eta_1 \eta_3 \frac{c_L}{c_D} \left(1 + \frac{\varphi}{1 - \varphi} \right) \int_{t_{end}}^{t_{start}} \frac{\left(\frac{dE_f}{dt} \right)}{\left(W_{OE} + W_{PL} + \frac{g}{e_{bat}} E_{0,bat} + \frac{g}{e_f} E_f(t) \right)} dt \tag{24}$$

Using the following differentiation rule:

$$\frac{d(lnx)}{dt} = \frac{1}{x} \frac{dx}{dt} \tag{25}$$

where x, in this case, is:

$$x = W_{OE} + W_{PL} + \frac{g}{e_{bat}} E_{0,bat} + \frac{g}{e_f} E_f(t) \tag{26}$$

Equation (24) becomes:

$$R = \eta_1 \eta_3 \frac{c_L}{c_D} \left(1 + \frac{\varphi}{1 - \varphi} \right) \int_{t_{end}}^{t_{start}} \left(\frac{e_f}{g} \right) \frac{d}{dt} \ln \left(W_{OE} + W_{PL} + \frac{g}{e_{bat}} E_{0,bat} + \frac{g}{e_f} E_f(t) \right) dt \tag{27}$$

$$R = \eta_1 \eta_3 \frac{c_L}{c_D} \left(1 + \frac{\varphi}{1 - \varphi}\right) \left(\frac{e_f}{g}\right) \ln \left(\frac{W_{OE} + W_{PL} + \frac{g}{e_{bat}} E_{0,bat} + \frac{g}{e_f} E_f(t_{start})}{W_{OE} + W_{PL} + \frac{g}{e_{bat}} E_{0,bat} + \frac{g}{e_f} E_f(t_{end})}\right) \tag{28}$$

$$E_f(t_{end}) = 0 \tag{29}$$

(As it is considered that the entire fuel (without reserves) is exhausted at the end of the flight) Equation (2) can be written as:

$$\varphi = \frac{P_{bat}\eta_2}{P_f\eta_1 + P_{bat}\eta_2} = \frac{P_{bat}\eta_2}{P_3} = \frac{E_{bat}\eta_2}{E_{o,tot}} \tag{30}$$

$$P_3 = P_f\eta_1 + P_{bat}\eta_2 \tag{31}$$

Converting power to energies, we obtain:

$$E_{o,tot} = E_f\eta_1 + E_{bat}\eta_2 \tag{32}$$

From Equations (30) and (32):

$$\varphi E_{o,tot} = E_{bat}\eta_2 \tag{33}$$

$$\varphi\left(E_f\eta_1 + E_{bat}\eta_2\right) = E_{bat}\eta_2 \tag{34}$$

Rearranging the above equation, we get:

$$E_f = E_{bat}\left(\frac{1 - \varphi}{\varphi}\right)\left(\frac{\eta_2}{\eta_1}\right) \tag{35}$$

Substituting from Equations (29) and (35) in Equation (28), we obtain:

$$R = \eta_1 \eta_3 \frac{c_L}{c_D} \left(1 + \frac{\varphi}{1 - \varphi}\right) \left(\frac{e_f}{g}\right) \ln \left(\frac{W_{OE} + W_{PL} + \frac{g}{e_{bat}} E_{bat} + \frac{g}{e_f} E_f(t_{start})}{W_{OE} + W_{PL} + \frac{g}{e_{bat}} E_{bat}}\right) \tag{36}$$

$$R = \eta_1 \eta_3 \frac{c_L}{c_D} \left(1 + \frac{\varphi}{1 - \varphi}\right) \left(\frac{e_f}{g}\right) \ln \left(\frac{W_{OE} + W_{PL} + \frac{g}{e_{bat}} E_{bat} + \frac{g}{e_f} E_{bat}\left(\frac{1-\varphi}{\varphi}\right)\left(\frac{\eta_2}{\eta_1}\right)}{W_{OE} + W_{PL} + \frac{g}{e_{bat}} E_{bat}}\right) \tag{37}$$

Using Equation (33), we get:

$$R = \eta_1 \eta_3 \frac{c_L}{c_D} \left(1 + \frac{\varphi}{1 - \varphi}\right) \left(\frac{e_f}{g}\right) \ln \left(\frac{W_{OE} + W_{PL} + \frac{g}{e_{bat}} \frac{\varphi E_{o,tot}}{\eta_2} + \frac{g}{e_f} \frac{\varphi E_{o,tot}}{\eta_2}\left(\frac{1-\varphi}{\varphi}\right)\left(\frac{\eta_2}{\eta_1}\right)}{W_{OE} + W_{PL} + \frac{g}{e_{bat}} \frac{\varphi E_{o,tot}}{\eta_2}}\right) \tag{38}$$

$$R = \eta_1 \eta_3 \frac{c_L}{c_D} \left(1 + \frac{\varphi}{1 - \varphi}\right) \left(\frac{e_f}{g}\right) \ln \left(\frac{W_{OE} + W_{PL} + E_{o,tot} g \left(\frac{\varphi}{e_{bat}\eta_2} + \frac{1-\varphi}{e_f\eta_1}\right)}{W_{OE} + W_{PL} + \frac{g}{e_{bat}} \frac{\varphi E_{o,tot}}{\eta_2}}\right) \tag{39}$$

$$R = \eta_1 \eta_3 \frac{c_L}{c_D} \left(1 + \frac{\varphi}{1 - \varphi}\right) \left(\frac{e_f}{g}\right) \ln \left(\frac{W_{OE} + W_{PL} + \left(\frac{E_{o,tot} g}{e_{bat}}\right) \left(\frac{\varphi}{\eta_2} + \frac{e_{bat}(1-\varphi)}{e_f\eta_1}\right)}{W_{OE} + W_{PL} + \frac{g}{e_{bat}} \frac{\varphi E_{o,tot}}{\eta_2}}\right) \tag{40}$$

Using the relation of efficiencies from Table 1, we get the following:

For parallel hybrid-electric aircraft:

$$R_{parallel} = \eta_{gt}\eta_{gb}\eta_p \frac{c_L}{c_D}\left(1 + \frac{\varphi}{1-\varphi}\right)\left(\frac{e_f}{g}\right)\ln\left(\frac{W_{OE} + W_{PL} + \left(\frac{E_{o,tot}g}{e_{bat}}\right)\left(\frac{\varphi}{\eta_{em}} + \frac{e_{bat}(1-\varphi)}{e_f\eta_{gt}}\right)}{W_{OE} + W_{PL} + \frac{g}{e_{bat}}\frac{\varphi E_{o,tot}}{\eta_{em}}}\right) \qquad (41)$$

For series hybrid-electric aircraft:

$$R_{series} = \eta_{gt}\eta_{eg}\eta_{em}\eta_{gb}\eta_p \frac{c_L}{c_D}\left(1 + \frac{\varphi}{1-\varphi}\right)\left(\frac{e_f}{g}\right)\ln\left(\frac{W_{OE} + W_{PL} + \left(\frac{E_{o,tot}g}{e_{bat}}\right)\left(\varphi + \frac{e_{bat}(1-\varphi)}{e_f\eta_{gt}\eta_{eg}}\right)}{W_{OE} + W_{PL} + \frac{g\varphi E_{o,tot}}{e_{bat}}}\right) \qquad (42)$$

Limiting cases:

Having derived the general equation and shown how these are reflected in the parallel and series hybrid-electric versions, the following exercise aims to show the three points:

- $\eta = 1$, to check if the new range Equation (40) reduces back to the range equation in [11];
- $\varphi = 0$, to check if the new range Equation (40) reduces back to the classical Brequet equation for a fully-fueled aircraft;
- $\varphi = 1$, to check if the new range Equation (40) reduces back to the range equation for a fully-electric aircraft.

Extreme efficiency case or $\eta = 1$:

Substituting $\eta = 1$ in Equation (40), we obtain:

$$R = \frac{c_L}{c_D}\left(1 + \frac{\varphi}{1-\varphi}\right)\left(\frac{e_f}{g}\right)\ln\left(\frac{W_{OE} + W_{PL} + \left(\frac{E_{o,tot}g}{e_{bat}}\right)\left(\varphi + \frac{e_{bat}(1-\varphi)}{e_f}\right)}{W_{OE} + W_{PL} + \frac{g}{e_{bat}}\varphi E_{o,tot}}\right)$$

The limiting case for $\eta = 1$ shows that the new efficiency-based hybrid-electric range equation is reduced to the hybrid-electric range equation derived in [11].

Fully-fueled case or $\varphi = 0$:

Substituting $\varphi = 0$ in Equation (40), we obtain:

$$R = \eta_1\eta_3 \frac{c_L}{c_D}\left(\frac{e_f}{g}\right)\ln\left(\frac{W_{OE} + W_{PL} + \frac{E_{o,tot}g}{e_f\eta_1}}{W_{OE} + W_{PL}}\right) \qquad (43)$$

Therefore, the limiting case for $\varphi = 0$ shows that the hybrid-electric range equation is reduced to the classical Brequet equation.

Fully-electric case or $\varphi = 1$:

The Equation (40) can be transformed into:

$$\lim_{\varphi=1}\frac{\ln\left(\frac{W_{OE}+W_{PL}+\left(\frac{E_{o,tot}g}{e_{bat}}\right)\left(\frac{\varphi}{\eta_2} + \frac{e_{bat}(1-\varphi)}{e_f\eta_1}\right)}{W_{OE}+W_{PL}+\frac{g}{e_{bat}}\frac{\varphi E_{o,tot}}{\eta_2}}\right)}{\frac{1}{\eta_1\eta_3\frac{c_L}{c_D}\left(1+\frac{\varphi}{1-\varphi}\right)\left(\frac{e_f}{g}\right)}} \qquad (44)$$

which is the indeterminate form $\frac{0}{0}$.

Applying the L'Hopitals rule [23] for solving indeterminate limits:

$$\lim_{\varphi=1} R = \frac{\frac{d(num)}{d\varphi}}{\frac{d(deno)}{d\varphi}} \qquad (45)$$

From Equation (44), the numerator can be written as:

$$\frac{d(num)}{d\varphi} = \frac{d\left(\ln\left(\frac{W_{OE}+W_{PL}+\left(\frac{E_{o,tot}g}{e_{bat}}\right)\left(\frac{\varphi}{\eta_2}+\frac{e_{bat}(1-\varphi)}{e_f\eta_1}\right)}{W_{OE}+W_{PL}+\frac{g}{e_{bat}}\frac{\varphi E_{o,tot}}{\eta_2}}\right)\right)}{d\varphi} \tag{46}$$

Using the following derivation rules:

$$\frac{d(lnx)}{dx} = \frac{1}{x} \tag{47}$$

$$\frac{d}{dx}\left(\frac{u}{v}\right) = \frac{v\frac{du}{dx} - u\frac{dv}{dx}}{v^2} \tag{48}$$

The Equation (46) can be written as:

$$\frac{d(num)}{d\varphi} = \frac{-\frac{g}{e_f}\frac{E_{o,tot}}{\eta_1}\left(W_{OE}+W_{PL}+\frac{g}{e_{bat}}\frac{E_{o,tot}}{\eta_2}\right)}{\left(W_{OE}+W_{PL}+\left(\frac{E_{o,tot}g}{e_{bat}}\right)\left(\frac{\varphi}{\eta_2}+\frac{e_{bat}(1-\varphi)}{e_f\eta_1}\right)\right)\left(W_{OE}+W_{PL}+\frac{g}{e_{bat}}\frac{\varphi E_{o,tot}}{\eta_2}\right)} \tag{49}$$

From Equation (44), the derivation of the denominator can be written as:

$$\frac{d(deno)}{d\varphi} = -\frac{1}{\eta_1\eta_3\frac{c_L}{c_D}\left(\frac{e_f}{g}\right)} \tag{50}$$

$$\lim_{\varphi=1} \frac{\frac{-\frac{g}{e_f}\frac{E_{o,tot}}{\eta_1}\left(W_{OE}+W_{PL}+\frac{g}{e_{bat}}\frac{E_{o,tot}}{\eta_2}\right)}{\left(W_{OE}+W_{PL}+\left(\frac{E_{o,tot}g}{e_{bat}}\right)\left(\frac{\varphi}{\eta_2}+\frac{e_{bat}(1-\varphi)}{e_f\eta_1}\right)\right)\left(W_{OE}+W_{PL}+\frac{g}{e_{bat}}\frac{\varphi E_{o,tot}}{\eta_2}\right)}}{-\frac{1}{\eta_1\eta_3\frac{c_L}{c_D}\left(\frac{e_f}{g}\right)}} \tag{51}$$

Finding the limit at $\varphi = 1$, we get:

$$R = \eta_3\frac{c_L}{c_D}\frac{E_{o,tot}}{\left(W_{OE}+W_{PL}+\frac{g}{e_{bat}}\frac{E_{o,tot}}{\eta_2}\right)} \tag{52}$$

Using Equations (22) and (33), we get:

$$R = \eta_2\eta_3\frac{c_L}{c_D}\frac{e_{bat}}{g}\frac{W_{bat}}{(W_{OE}+W_{PL}+W_{bat})} \tag{53}$$

Therefore, the limiting case for $\varphi = 1$ shows that the hybrid-electric range equation is reduced to the electric aircraft range equation.

Having shown the derivation of the new efficiency-based hybrid-electric range equation and its validation using the limiting cases, it is now applied to a case study in the section below.

5. Case Study

To demonstrate the dramatic impact that the correction of the definition of φ has, this paper will make use of the same case study worked out in [11]. We purposefully consider the same case study to show the effect that the new efficiency-based degree of hybridization has on the range. The input parameters are shown in Table 2. The results for a parallel hybrid and series hybrid configuration are shown in Figures 4 and 5, respectively.

Table 2. Input parameters for the case study.

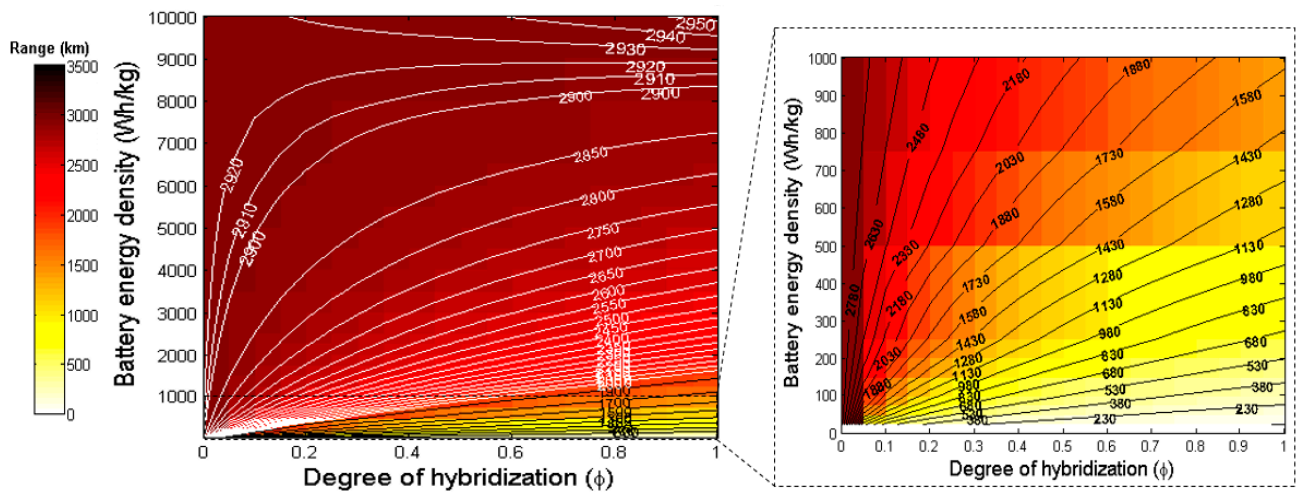| Variable	Value
Empty weight (W_{OE} [N])	50,000
Payload weight (W_{PL} [N])	20,000
Total input energy ($E_{o,tot}$ [GJ])	25
Lift-to-drag ratio (*L/D* ratio)	12
Gas turbine efficiency (η_{gt})	0.35
Electric motor efficiency (η_{em})	0.95
Electric generator efficiency (η_{eg})	0.98
Propulsive efficiency (η_p)	0.80
Gearbox efficiency (η_{gb})	0.95
Energy density of aviation fuel (e_f [Wh/kg])	11,900
Acceleration due to gravity (g [m/s^2])	9.81

Figure 4. Aircraft range (km) as a function of battery energy density and degree of hybridization for the parallel-hybrid configuration. (Insert: Zoom in on battery energy density <1000).
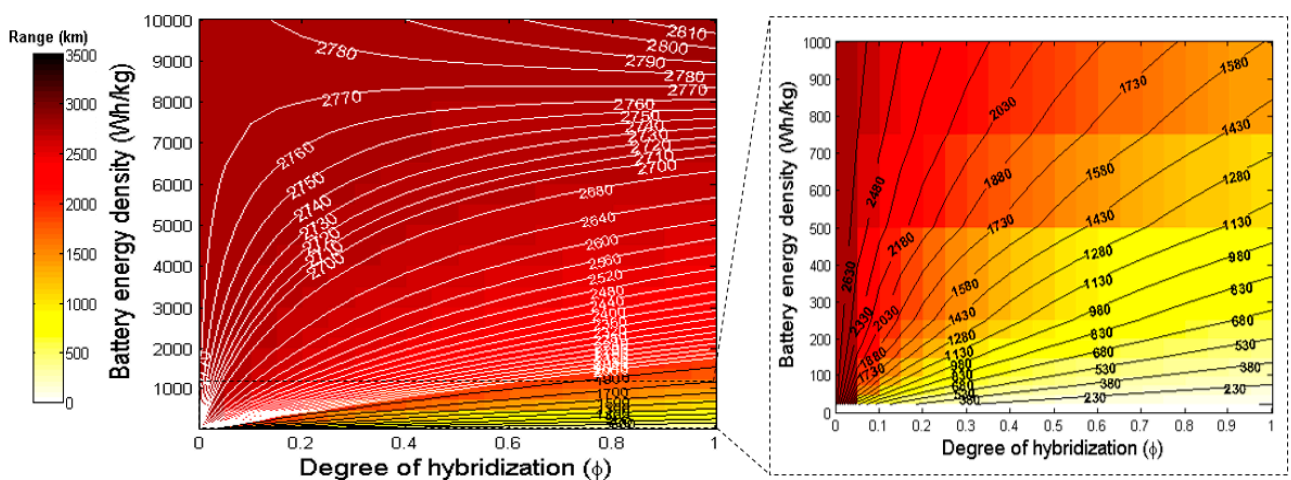

Figure 5. Aircraft range (km) as a function of battery energy density and degree of hybridization for the series-hybrid configuration. (Insert: Zoom in on battery energy density <1000).

From Figures 4 and 5, a number of observations can be made, namely:

- A parallel hybrid-electric configuration provides a slightly higher range than a series hybrid-electric configuration. This is largely due to the fact that a series hybrid electric has a double efficiency penalty on the electric powertrain, one on the generator and one on the motor. Conversely, the series hybrid only requires the motor powered by the battery and therefore does not suffer from this penalty. The difference between the two configurations increases with an increased degree of hybridization. In order to highlight the differences between the two configurations, some point data were selected and are listed in Table 3 below.

Table 3. Point data highlighting differences in aircraft range between series and parallel hybrid-electric configurations.

		Parallel Configuration		Series Configuration	
	Battery Energy Density	**400 Wh/kg**	**800 Wh/kg**	**400 Wh/kg**	**800 Wh/kg**
Degree of hybridization	**0.3**	1761.7 km	2224.2 km	1707.6 km	2138.7 km
	0.6	1260.9 km	1795 km	1234.2 km	1741.1 km
	0.9	982.1 km	1505 km	966.5 km	1468.7 km

- For both parallel and series-hybrid configurations, with a constant battery energy density, the range decreases with an increase in the degree of hybridization. This is observed to happen until a threshold in battery energy density is reached. Beyond this threshold, the aircraft range increases with the degree of hybridization. This follows the logical sequence that below the threshold, the battery energy density is still too low compared with fuel energy density; with an increase in the degree of hybridization, the weight of batteries would increase, therefore, the resultant range decreases. However, as the product of the battery energy density and powertrain efficiencies become comparable to the product of the fuel energy density and combustion efficiency, the range of the aircraft increases with a higher degree of hybridization towards the full electric aircraft.

- This threshold value is the point at which the aircraft range becomes independent of the degree of hybridization. In Parallel hybrid-electric, this threshold is at 9300 Wh/kg, while in series hybrid-electric configurations, this threshold is at 8700 Wh/kg. The larger value for a parallel hybrid-electric is also logical, as this configuration has a stronger dependence on the battery. The actual values change depending on the aircraft parameters chosen in Table 2. However, in our work we specifically choose the same values used in earlier research [11] to show that there is now a strong departure from the earlier published research, which showed a threshold of 500 Wh/kg. This is a direct effect of the definition of the efficiency-based degree of hybridization, which now also takes into consideration the efficiencies of the fuel and electric powertrains. Due to the change in threshold from [11], the differences were observed in the results of the range as well.

- The significance of the much larger threshold values becomes apparent when taken into context. Battery energy density doubles approximately every 23 years [5]. Considering that the current state-of-the-art battery technology has an energy density of 228 Wh/kg, the old definition makes a hybrid aircraft with properties specified in Table 2 achievable within the next two decades. However, when considering all efficiencies, this threshold lies beyond the theoretical limits of battery energy densities (228 Wh/kg).

- Despite the significant progress in battery technology required to enable electric flight, hybrid electric aircraft may still be applied to smaller aircraft which do not exceed the 1000 km range. An example of this is in the use of regional aircraft. Even a low degree of hybridization, when applied to a large fleet, would offer a significant reduction in

fuel consumption and emissions. Therefore, the authors feel that this hybrid-electric configuration has the ability to bridge the gap until better fuel alternatives are found.

6. Conclusions

This paper derives a new equation for the range of hybrid-electric aircraft. The paper revisits the existing range equation for hybrid-electric aircraft [11] and proposes an efficiency-based definition of the degree of hybridization φ. The efficiency of the power train is an important element of the conversion from energy into propulsive power. In our definition, we therefore introduce the effect of the combustion efficiency and the efficiency of the electric powertrain. In our work, we find that this change in the definition of φ has a significant impact on the range equation. The paper also shows how when considering the limiting factor for $\varphi = 0$ (fully fuel powered) and $\varphi = 1$ (fully electric-powered), the range equation reduces to the classical Breguet equation and the electric aircraft range, respectively. Finally, the paper considers a case study to show the full impact of the change in the definition of φ and the resulting range equation. We show that for every aircraft design, there is a battery energy threshold for which the range becomes independent of the degree of hybridization. Below this threshold, the aircraft range decreases with an increase in the degree of hybridization. On the other hand, above this battery energy density threshold, the aircraft range increases with an increase in the degree of hybridization. Despite this, the authors feel that hybrid-electric aircraft can still contribute to the shift towards net zero. Even aircraft with a low degree of hybridization can offer significant savings in fuel and emissions. Hybrid-electric aircraft can therefore play an important role in bridging the gap until cleaner fuel alternatives are achieved.

Author Contributions: Conceptualization, A.B., R.R. and R.C.; data curation, A.B.; formal analysis, A.B., R.R. and R.C.; funding acquisition, R.C.; investigation, A.B., R.R. and R.C., methodology, A.B. and R.R.; project administration, R.C.; supervision, R.C. and R.R.; resources, R.C.; visualization, A.B.; validation, R.C.; writing—original draft preparation, A.B.; writing—review and editing, R.C. and R.R. All authors have read and agreed to the published version of the manuscript.

Conflicts of Interest: The authors declare no conflict of interest.

Nomenclature

c_L	Coefficient of Lift
c_D	Coefficient of Drag
D	Drag [N]
e	Specific Energy [J/kg]
E	Energy [J]
g	Gravitational acceleration [m/s^2]
L	Lift [N]
P	Power [W]
R	Range [m]
S	Planform area [m^2]
t	Time [s]
T	Thrust [N]
v	Velocity [m/s]
W	Weight [N]
γ	Flight path angle [rad]
η	Efficiency
φ	Degree of hybridization
ρ	Density

Subscripts

1,2,3	Powertrain branch indices
bat	Battery
eg	Electrical generator
em	Electrical motor
end	End of mission segment
f	Fuel
gt	Gas turbine
gb	Gearbox
OE	Operating Empty
p	Propeller
PL	Payload
start	Start of mission segment
tot	Total

References

1. Airbus Global Market Forecast (GMF). Available online: https://www.airbus.com/en/products-services/commercial-aircraft/market/global-market-forecast (accessed on 15 July 2023).
2. European Commission. Flightpath 2050 CARE2050. Flightpath 2050, Europe's Vision for Aviation. Available online: https://ec.europa.eu/transport/sites/transport/files/modes/air/doc/flightpath2050.pdf (accessed on 2 December 2022).
3. Hoelzen, J.; Silberhorn, D.; Zill, T.; Bensmann, B.; Rauschenbach, R.H. *Hydrogen-Powered Aviation and Its Reliance on Green Hydrogen Infrastructure—Review and Research Gaps*; Elsevier: Amsterdam, The Netherlands, 2022; Volume 47, No. 5, pp. 3108–3130. [CrossRef]
4. Schwab, A.; Thomas, A.; Bennett, J.; Robertson, E.; Cary, S. *Electrification of Aircraft: Challenges, Barriers, and Potential Impacts*; NREL/TP-6A20-80220; National Renewable Energy Laboratory (NREL): Golden, CO, USA, 2021.
5. Zhang, L.; Butler, T.L.; Yang, B. Recent Trends, Opportunities and Challenges of Sustainable Aviation Fuel. In *Green Energy to Sustainability: Strategies for Global Industries*, 1st ed.; Wiley: New York, NY, USA, 2020.
6. Viswanathan, V.; Epstein, A.H.; Chiang, Y.; Takeuchi, E.; Bradley, M.; Langford, J.; Winter, M. The challenges and opportunities of battery-powered flight. *Nat. Perspect.* **2022**, *601*, 519–525. [CrossRef] [PubMed]
7. International Food Policy Research Institute (IFPRI). F00d Versus Fuel v2.0: Biofuel Policies and the Current Food Crisis. Available online: https://www.ifpri.org/blog/food-versus-fuel-v20-biofuel-policies-and-current-food-crisis (accessed on 16 July 2023).
8. Rossi, N.; Trainelli, L.; Riboldi, C.E.D.; Rolando, A. Conceptual Design of Hybrid-Electric Aircraft. Politech. Di Milano 2018, 2016–2017. Available online: https://www.politesi.polimi.it/bitstream/10589/139491/3/2018_04_Rossi.pdf (accessed on 16 July 2023).
9. Wheeler, P.; Sirimanna, A.S.; Bozhko, S.; Haran, K.S. Electric/Hybrid-Electric Aircraft Propulsion Systems. *Proc. IEEE* **2021**, *109*, 1115–1127. [CrossRef]
10. Marciello, V.; Ruocco, M.; Nicolosi, F.; Stasio, M.D. Markey Analysis, TLARS selection and preliminary design investigations for a regional hybrid-electric aircraft. In Proceedings of the 33rd Congress of the International Council of the Aeronautical Sciences (ICAS), Stockholm, Sweden, 4–9 September 2022.
11. Vries, R.D.; Hoogreef, M.F.M.; Vos, R. Range Equation for Hybrid-Electric Aircraft with Constant Power Split. *J. Aircr.* **2020**, *57*, 552–557. [CrossRef]
12. Raymer, D.P. *Aircraft Design: A Conceptual Approach*; AIAA Education Series; AIAA: Reston, VA, USA, 2002. [CrossRef]
13. Hepperle, M. Electric Flight—Potential and Limitations. NATO Report STO-MP-AVT-209. 2012. Available online: https://elib.dlr.de/78726/1/MP-AVT-209-09.pdf. (accessed on 16 July 2023).
14. Ravishankar, R.; Chakravarthy, S.R. Range Equation for a Series Hybrid Electric Aircraft. In Proceedings of the 2018 Aviation Technology, Integration, and Operations Conference, Atlanta, GA, USA, 25–29 June 2018. [CrossRef]
15. Elmousadik, S.; Ridard, V.; Sécrieru, N.; Joksimovic, A.; Maury, C.; Carbonneau, X. New Preliminary Sizing Methodology for a Commuter Airplane with Hybrid-Electric Distributed Propulsion. In Proceedings of the Advanced Aircraft Efficiency in a Global Air Transport System (AEGATS 18), Toulouse, France, 23–25 October 2018.
16. Rohacs, J.; Rohacs, D. Energy coefficients for comparison of aircraft supported by different propulsion systems. *Energy* **2019**, *191*, 1–11. [CrossRef]
17. Marwa, M.; Martin, S.M.; Martos, B.C.; Anderson, R.P. Analytic and Numeric Forms for the Performance of Propeller-Powered Electric and Hybrid Aircraft. In Proceedings of the 55th AIAA Aerospace Sciences Meeting, Grapevine, TX, USA, 9–13 January 2017. [CrossRef]
18. Hartmann, J.; Strack, M.; Nagel, B. Conceptual Assessment of Different Hybrid Electric Air Vehicle Options for a Commuter with 19 Passengers. In Proceedings of the 2018 AIAA Aerospace Sciences Meeting, Kissimmee, FL, USA, 8–12 January 2018. [CrossRef]
19. Xie, Y.; Savvarisal, A.; Tsourdos, A.; Zhang, D.; Gu, L. Review of hybrid electric powered aircraft, its conceptual design and energy management methodologies. *Chin. J. Aeronaut.* **2020**, *34*, 432–450. [CrossRef]

20. Finger, D.F.; Braun, C.; Bil, C. Comparative Assessment of Parallel-Hybrid-Electric Propulsion Systems for Four Different Aircraft. *J. Aircr.* **2020**, *57*, 843–853. [CrossRef]

21. Zamboni, J.; Vos, R.; Emeneth, M.; Schneegans, A. A Method for the Conceptual Design of Hybrid Electric Aircraft. In Proceedings of the AIAA SciTech 2019 Forum, San Diego, CA, USA, 7–11 January 2019. [CrossRef]

22. Bai, M.; Yang, W.; Li, J.; Kosuda, M.; Fozo, L.; Kelemen, M. Sizing methodology and Energy Management of an Air-Ground Aircraft with Turbo-Electric Hybrid Propulsion System. *Aerospace* **2022**, *9*, 764. [CrossRef]

23. Taylor, A.E. L'Hospital's Rule. *Am. Math. Mon.* **1952**, *59*, 20–24. [CrossRef]